Paper

Projected Cancer Risks to Residents of New Mexico from Exposure to Trinity Radioactive Fallout

Elizabeth K. Cahoon,[1] Rui Zhang,[1] Steven L. Simon,[1] André Bouville,[2] and Ruth M. Pfeiffer[1]

Abstract—The Trinity nuclear test, conducted in 1945, exposed residents of New Mexico to varying degrees of radioactive fallout. Companion papers in this issue have detailed the results of a dose reconstruction that has estimated tissue-specific radiation absorbed doses to residents of New Mexico from internal and external exposure to radioactive fallout in the first year following the Trinity test when more than 90% of the lifetime dose was received. Estimated radiation doses depended on geographic location, race/ethnicity, and age at the time of the test. Here, these doses were applied to sex- and organ-specific risk coefficients (without applying a dose and dose rate effectiveness factor to extrapolate from a population with high-dose/high-dose rates to those with low-dose/low-dose rates) and combined with baseline cancer rates and published life tables to estimate and project the range of radiation-related excess cancers among 581,489 potentially exposed residents of New Mexico. The total lifetime baseline number of all solid cancers [excluding thyroid and non-melanoma skin cancer (NMSC)] was estimated to be 183,000 from 1945 to 2034. Estimates of ranges of numbers of radiation-related excess cancers and corresponding attributable fractions from 1945 to 2034 incorporate various sources of uncertainty. We estimated 90% uncertainty intervals (UIs) of excess cancer cases to be 210 to 460 for all solid cancers (except thyroid cancer and NMSC), 80 to 530 for thyroid cancer, and up to 10 for leukemia (except chronic lymphocytic leukemia), with corresponding attributable fractions ranging from 0.12% to 0.25%, 3.6% to 20%, and 0.02% to 0.31%, respectively. In the counties of Guadalupe, Lincoln, San Miguel, Socorro, and Torrance, which received the greatest fallout deposition, the 90% UI for the projected fraction of thyroid cancers attributable to radioactive fallout from the Trinity test was estimated to be from 17% to 58%. Attributable fractions for cancer types varied by race/ethnicity, but 90% UIs overlapped for all race/ethnicity groups for each cancer grouping. Thus, most cancers that have occurred or will occur among persons exposed to Trinity fallout are likely to be cancers unrelated to exposures from the Trinity nuclear test. While these ranges are based on the most detailed dose reconstruction to date and rely largely on methods previously established through scientific committee agreement, challenges inherent in the dose estimation, and assumptions relied upon both in the risk projection and incorporation of uncertainty are important limitations in quantifying the range of radiation-related excess cancer risk.
Health Phys. 119(4):478–493; 2020
Key words: cancer; fallout; nuclear weapons; radiation risk

[1]Division of Cancer Epidemiology & Genetics, National Cancer Institute, National Institutes of Health, Bethesda, MD; [2]Retired (NCI/NIH).

For correspondence contact Elizabeth K. Cahoon, Radiation Epidemiology Branch, DCEG, National Cancer Institute, NIH, DHHS, 9609 Medical Center Drive, Rm 7E452, MS 9778, Bethesda, MD 20892-9778, or email at cahoonek@mail.nih.gov; or Ruth M. Pfeiffer, Biostatistics Branch, DCEG, National Cancer Institute, NIH, DHHS, 9609 Medical Center Dr., Rm 7E142, Bethesda, MD 20892-9778 or email at pfeiffer@mail.nih.gov.

INTRODUCTION

THE TRINITY nuclear test was conducted on 16 July 1945 in south-central New Mexico as the culmination of the Manhattan Project, just 3 wk before the atomic bombings of Hiroshima and Nagasaki, Japan. The device was similar to the Fat Man-type plutonium implosion device used in the bombing of Nagasaki. The test resulted in varying levels of radiation dose from radioactive fallout to residents of New Mexico depending on geographic location of residence, age at the time of the test, and race/ethnicity. Because the test occurred over 70 y ago, it is not possible to retrospectively identify the population exposed and collect statewide records of the number and types of cancers that occurred in that population. For that reason, conducting an analytical epidemiological follow-up study of exposed individuals is not feasible.

Recognizing, however, that ionizing radiation is an established carcinogen, exposure of the New Mexico population could lead to an increase in cancer incidence. Information that quantitatively relates radiation dose levels to cancer risk is required to provide an estimate (and/or projection) of such an increase. Today, the best quantitative evaluation of radiation-related cancer risk as a function of radiation dose is based largely on epidemiological studies of the Japanese atomic bomb survivors who were acutely exposed to low to moderate/high external doses, in addition to some other radiation-exposed populations (Ron et al. 1995; NRC 2005; Preston et al. 2007). Cancer risk models developed using

data from the Japanese atomic bomb survivors can be used to estimate or project risks in other populations with different exposure scenarios; e.g., the residents of New Mexico alive at the time of the Trinity test. This extrapolation from one population to another adds uncertainty in estimating the impact of radiation on cancer risks, but in the absence of a large, well-defined and carefully followed cohort of Trinity fallout-exposed individuals with individual dose estimates, radiation risk projection based on models developed from other exposed cohorts remains the only viable tool to estimate the number of cancers that might have been caused by fallout exposure to the New Mexico population (NRC 2005; Berrington de Gonzalez et al. 2012).

Our objective is to estimate the range of radiation-related excess cancers and corresponding attributable fractions from exposure to fallout from the Trinity nuclear test among the residents of New Mexico alive at the time of the test. We use multiple databases to characterize the exposed New Mexico population and baseline cancer rates and statistical risk projection methods with reconstructed radiation doses (Simon et al. 2020) to estimate the potential magnitude and proportion of radiation-related cancer risks. We consider uncertainties of the models and other factors used in the calculations and describe limitations in the uncertainty analysis. This is the first assessment of cancer risks due to exposure to radioactive fallout from the Trinity nuclear test.

MATERIALS AND METHODS

Based on methods and data described in companion papers (Bouville et al. 2020; Potischman et al. 2020; Simon et al. 2020), estimates of tissue-specific radiation absorbed doses from exposure to fallout from external and internal sources were derived for residents of different precincts by age at the time of the test and race/ethnicity for the first year following the Trinity test. In the current paper, total (internal and external combined) tissue-specific radiation doses are applied to baseline cancer rates, published life tables, and sex- and organ-specific risk coefficients to project the number of excess cancers among residents of New Mexico alive at the time of the test.

Study population

The population residing in New Mexico at the time of the Trinity test on 16 July 1945 was estimated by linear interpolation of the 1940 and 1950 United States census counts and is presented in Table 1 (USCB 2019). The total number of people reported in 5-y age groups by the census were apportioned equally to single year ages within that 5-y group. For the wider age group of people 75 y and older, individuals were apportioned from ages 75 to 90 y based on 1939 US life tables for males and females. These censuses capture race/ethnicity of Whites, African Americans, and "other races." For New Mexico, the "other races"

Table 1. Distribution of the New Mexico population by age and race/ethnicity in 1945.

Age group (y)	White	Hispanic	Native American	African American	Total
0–4	38,816	27,764	5,544	467	72,591
5–9	36,029	25,770	4,432	444	66,674
10–14	33,692	24,099	3,599	406	61,797
15–19	30,691	21,952	3,094	423	56,160
20–24	28,079	20,084	3,367	524	52,053
25–29	28,169	20,148	2,952	755	52,024
30–34	24,609	17,602	2,287	607	45,105
35–39	21,401	15,308	1,993	549	39,251
40–44	17,424	12,463	1,533	494	31,915
45–49	15,335	10,969	1,149	407	27,859
50–54	12,139	8,682	1,166	265	22,252
55–59	9,176	6,563	929	162	16,830
60–64	6,757	4,833	862	163	12,614
65–69	5,537	3,960	520	127	10,143
70–74	3,671	2,626	553	69	6,919
75 and older	3,828	2,738	693	42	7,301
Total	315,352	225,561	34,673	5,903	581,489

category was assumed to be Native Americans.[3] The 1940 census combined counts for non-Hispanic whites and Hispanic whites for each county in New Mexico. However, a 5% sample of the 1940 census indicates that Hispanics (using the definition of having the Spanish mother tongue) represented 41.7% of the entire population of New Mexico at that time. We assumed the Hispanic population to be 41.7% of every precinct and age group combination, rounded to the nearest person. The total population of New Mexico in 1945 was estimated to be 581,489 people comprised of 315,352 Whites; 225,561 Hispanics; 34,673 Native Americans; and 5,903 African Americans.

Radiation dose

Tissue-specific absorbed doses (Table 2) from a range of radionuclides were estimated (Simon et al. 2020) for individuals residing in the 721 precincts of New Mexico for the primary organs at risk from exposure to radioactive fallout: active bone marrow, thyroid, stomach, colon, and lung, similar to analyses done for other populations exposed to radioactive fallout (Land et al. 2010). For the cancer risk projection of other organs, colon dose was used as a surrogate dose to project the excess of all solid cancers [excluding thyroid and non-melanoma skin cancer (NMSC)]. The dose reconstruction relied on fallout deposition estimates derived from ground-level exposure-rate measurements made within 3 wk of the detonation, which were later confirmed by measurements from environmentally-placed x-ray film badges (Hoffman 1945), and on recall of diet and lifestyle from

---

[3]The research findings in this paper do not apply to the Navajo Nation.

Table 2.[4] Adapted from Simon et al. (2020). Mean radiation absorbed doses (mGy) to residents of New Mexico from Trinity radioactive fallout by county and age at exposure groupings. Abbreviations: ABM, active bone marrow. Doses rounded to two significant digits. Note: Weighted by population size in corresponding county and age grouping during first year at risk (1950 for solid cancers and 1947 for leukemia).

Population	Age group (y)	ABM	Thyroid	Colon	Stomach	Lung
Total[a]						
	<1	7.2E-01	1.1E+01	3.1E+00	8.7E-01	2.8E+00
	1–2	8.2E-01	3.0E+01	4.9E+00	1.0E+00	2.4E+00
	3–7	6.8E-01	2.2E+01	3.1E+00	7.9E-01	1.7E+00
	8–12	6.7E-01	1.6E+01	3.0E+00	7.6E-01	1.8E+00
	13–17	6.3E-01	1.2E+01	2.5E+00	6.8E-01	1.8E+00
	Adult	4.8E-01	6.6E+00	2.1E+00	5.8E-01	1.6E+00
Selected counties[b]						
	<1	5.2E+00	6.6E+01	2.3E+01	6.5E+00	2.2E+01
	1–2	5.4E+00	1.7E+02	2.6E+01	6.8E+00	1.9E+01
	3–7	4.6E+00	1.3E+02	1.7E+01	5.5E+00	1.3E+01
	8–12	4.5E+00	9.1E+01	1.7E+01	5.3E+00	1.4E+01
	13–17	4.2E+00	6.8E+01	1.5E+01	4.9E+00	1.4E+01
	Adult	3.5E+00	3.9E+01	1.3E+01	4.2E+00	1.2E+01
Other counties						
	<1	9.7E-02	2.9E+00	3.2E-01	8.9E-02	1.3E-01
	1–2	1.8E-01	1.1E+01	2.0E+00	1.9E-01	1.7E-01
	3–7	1.3E-01	7.4E+00	1.2E+00	1.4E-01	1.4E-01
	8–12	1.4E-01	5.2E+00	1.1E+00	1.3E-01	1.5E-01
	13–17	1.4E-01	4.0E+00	7.6E-01	1.1E-01	1.4E-01
	Adult	8.1E-02	2.2E+00	5.7E-01	8.7E-02	1.1E-01

[a]Including precincts with doses estimated to be greater than zero.

[b]Including Guadalupe, Lincoln, San Miguel, Socorro, and Torrance.

the mid-1940s in contemporary focus groups and personal interviews from persons alive and residing in New Mexico at the time of Trinity. In the dose assessment, three exposure pathways were included: (1) external irradiation from the radionuclides deposited on the ground, (2) inhalation of radionuclide-contaminated air during and after the passage of the radioactive cloud, and (3) ingestion of contaminated water and food. The ingestion pathway accounted for radioactive contamination of 13 types of food and water (Bouville et al. 2020; Simon et al. 2020). The calculations of contamination of foods and air for the internal dose assessment accounted for 63 radionuclides in the fallout that are fission or activation products. Of the 63 considered, 54 have radioactive half-lives of less than 3 mo, while only nine have radioactive half-lives longer than 9 mo. The risk analysis presented here uses estimates of intakes and doses received in the first year following the test. Any dose received in later years would not only be much smaller than the component assessed but would also be considerably more uncertain. Each derived dose estimate was considered to be the "best estimate" of radiation absorbed dose to specific organs for persons representative of a specific age-at-exposure group (0 to <1 y, 1–2 y, 3–7 y, 8–12 y, 13–17 y, and 18 y and older) and race/ethnicity (Whites, Hispanics, Native Americans, and African

Americans) in each precinct. Different dietary and lifestyle patterns were assumed for each precinct based on collected data from interviews and focus groups (Potischman et al. 2020). Table 2, adapted from Simon et al. (2020), presents population-size weighted mean radiation absorbed doses by county and age at exposure groupings among residents of New Mexico alive in 1945 with doses estimated to be greater than zero.

Baseline cancer rates

Baseline cancer rates are cancer incidence rates in a population without known exposure to the factor of interest; in this case, radiation from Trinity fallout. Baseline incidence rates for each specific cancer type vary between populations as well as over calendar time, across ages, birth cohorts, sex, and race/ethnicity groups within a population. To ensure stable estimates of baseline cancer rates by age at diagnosis, calendar year, sex, and race/ethnicity, we used cancer incidence rates reported by the Surveillance, Epidemiology, and End Results (SEER) cancer registry program from 1973 to 2015, which includes between 9 and 18 high-quality cancer registries across the United States. To derive baseline cancer incidence rates for 1945 to 1972, we extrapolated rates for all races combined from 1973 to 1987 from the nine SEER cancer registries (SEER9 2018). We fit Poisson regression models that included 5-y age groups

[4]E-notation is used here due to space restrictions.

coded with dummy variables [combining 0 to 10-y-olds for thyroid, leukemia—except chronic lymphocytic leukemia (CLL)], solid (except thyroid and NMSC) and 0 to 15-y-olds for lung, colon, and stomach cancer), calendar year in single years fitted as a continuous variable, sex, and interaction terms of calendar year by sex and age groups by sex. The SEER program includes cancer incidence rates for individuals of Hispanic ethnicity since 1992, so race ratios of Hispanics/Blacks/non-HispanicWhites/NativeAmericans compared to all races combined estimated using SEER rates from 1992 to 2006 were applied to cancer incidence rates for earlier periods. Poisson regression models using SEER 18 data from 2000 to 2015 were used to extrapolate age-, sex-, and race/ethnicity-specific cancer incidence rates to years 2016 to 2034. Further details are provided in Appendix A.

Models for estimating radiation-related cancer risk

Excess radiation-related cancer risk can be computed either based on a multiplicative model with the excess relative risk (ERR), an additive model using the excess absolute risk (EAR), or a combination of the two models. We used models based on the recommendations of the National Academy of Sciences BEIR VII report on the Biological Effects of Ionizing Radiation (NRC 2005). BEIR VII dose-response models were used for estimating the ERR and EAR per unit dose of radiation (Table 3). Most of the radiation dose-response coefficients in the BEIR VII report (denoted by β, γ, η, δ, and φ in the equation below) are based on analyses of data from the Life Span Study of Japanese atomic bomb survivors, which is considered the gold standard in radiation risk assessment (Preston et al. 2007). The general form of the BEIR VII dose-response models for the ERR and EAR is

$$ERR(D, s, e, a, t) \; or \; EAR(D, s, e, t)$$
$$= \beta_s D exp(\gamma e + \eta a + \delta t + \varphi et). \qquad (1)$$

Here, D is dose in Gy, e = (exposure age-30)/10 for exposure age<30 and e = 0 for exposure age $\geq$ 30, a = $\log_e$ (attained age/60) and t = $\log_e$(time since exposure/25), where time since exposure in years is attained by age minus age at exposure. Age in years at exposure in this study is defined as age at the time of the Trinity test. For example, based on these models (eqn 1) and coefficients (Table 3), the radiation-related risk of thyroid cancer is only modified by age at exposure, with a stronger modification than other cancers; thus, decreasing age at exposure substantially increases thyroid cancer risk. The dose-response model for leukemia (excluding CLL) described in BEIR VII has a linear-quadratic form for acute exposures, but the quadratic term is typically dropped for protracted exposures, like those due to radioactive fallout (Land et al. 2010). We also used the BEIR VII committee's assumptions for cancer latency, that

cancer risk follows a step function so that it is equal to zero at time since exposure of less than 2 y for leukemia and less than 5 y for solid cancers. Unlike the BEIR VII report, we did not apply a dose and dose rate effectiveness factor (DDREF) to extrapolate from populations with high-dose/high-dose rates to those with low-dose/low-dose rates. A DDREF greater than 1, when applied to the excess relative risk, would reduce the number of estimated excess cases.

Transfer of estimated excess relative risk to the exposed New Mexico population

Selection of the weight given to the ERR and EAR models can significantly impact the projected excess cancer risk when the baseline cancer rates differ between the population from which the ERR or EAR was derived (e.g., Japanese atomic bomb survivors) and the population to which the risk is transferred (e.g., 1945 residents of New Mexico). The BEIR VII approach uses the multiplicative model (i.e., ERR) for thyroid cancer because mechanistic considerations suggest greater support for relative risk than for absolute risk transport (NRC 2005). For leukemia (except CLL), stomach cancer, colon cancer, and for solid cancers (except thyroid and NMSC), the BEIR VII approach uses a weighted average (on the logarithmic scale) of the ERR and EAR models with weights of 0.7 on multiplicative transfer (ERR) and 0.3 on additive transfer (EAR). For lung cancer, the multiplicative model (ERR) weight is 0.3 and 0.7 for the additive (EAR) model. We used a similar approach, except that the weighted averages are on the arithmetic, rather than the logarithmic, scale as used by previous studies to enable propagation of uncertainties (Land et al. 2010; Berrington de Gonzalez et al. 2012).

Person-years

The models recommended by BEIR VII provide estimates of the age-specific excess cancer risks. However, projected lifetime cancer risk must reflect person-time at risk over the lifespan. Here, we use the term "person-years" to represent the sum of years for which the study population is at risk of developing cancer. Person-years at risk reflect the conditional probability of a person reaching a certain age. United States (US) life tables provide 1-y survival data for persons alive at any given age during that calendar period and are published approximately every 10 y, based largely on US census data (CDC 2019). We assumed that individuals in the exposed population could reach an age of up to 90 years and estimated person-years from age in 1945 up until age 90 y or year 2034 using published life tables by calendar year, sex, and race/ethnicity, when available. For each corresponding sex, race/ethnicity, calendar year, and age, we multiplied the corresponding baseline cancer rates by the person-years for that age and summed over the different ages to estimate lifetime cancer risk. This approach adjusts for competing age-specific mortality in estimating cumulative

Table 3. Estimates (95% uncertainty limits) of preferred ERR and EAR model parameters for estimating site-specific cancer risk. Abbreviations: ERR, excess relative risk; EAR, excess absolute risk; PY, person-years.

Model parameter	Leukemia[a]	Thyroid	Colon	Stomach	Lung	All solid[b]
ERR[d]						
β_M	1.1 (0.10, 2.6)	0.53 (0.14, 2.0)	0.63 (0.37, 1.1)	0.21 (0.11, 0.40)	0.32 (0.15, 0.70)	0.33 (0.24, 0.47)
β_F	1.2 (0.10, 2.9)	1.05 (0.28, 3.9)	0.43 (0.19, 0.96)	0.48 (0.31, 0.73)	1.40 (0.94, 2.1)	0.57 (0.44, 0.74)
$\gamma(e)$	-0.4 (-0.78, 0.0)	-0.83[c]	-0.3[c]	-0.3[c]	-0.3[c]	-0.3 (-0.51, -0.10)
$\eta(a)$	0	0	-1.4[c]	-1.4[c]	-1.4[c]	-1.4 (-2.2, -0.7)
$\delta(t)$	-0.48 (-1.1, 0.20)	0	0	0	0	0
$\varphi(e*t)$	0.42 (0.0, 0.96)	0	0	0	0	0
EAR (per 10^4 PY)[d]						
β_M	1.62 (0.1, 3.6)	0	3.2 (1.8, 5.6)	4.9 (2.7, 8.9)	2.3 (1.1, 5.0)	22 (15, 30)
β_F	0.93 (0.1, 2.0)	0	1.6 (0.8, 3.2)	4.9 (3.2, 7.3)	3.4 (2.3, 4.69)	28 (22,36)
$\gamma(e)$	0.29 (0.0, 0.62)	0	-0.41[c]	-0.41[c]	-0.41[c]	-0.41 (-0.59, -0.22)
$\eta(a)$	0	0	2.8[c]	2.8[c]	5.2 (3.8, 6.6)	2.8 (2.15, 3.41)
$\delta(t)$	0	0	0	0	0	0
$\varphi(e*t)$	0.56 (0.31, 0.85)	0	0	0	0	0
Multiplicative/additive transfer weights	0.7/0.3	1.0/0.0	0.7/0.3	0.7/0.3	0.3/0.7	0.7/0.3

[a] Leukemia excludes CLL. Because dose from fallout was considered to have been received at a low dose rate, the parameter for the dose-squared term in the BEIR VII model for leukemia was set equal to zero.

[b] Except thyroid cancer and non-melanoma skin cancer.

[c] Error assumed to be negligible, following BEIR VII (NRC 2006).

[d] The form of the ERR and EAR models is $\beta_s D exp\, (\gamma e + \eta a + \delta t + \varphi et)$ where D is dose in Gy; (age at exposure-30)/10 for age at exposure<30 and e = 0 for age≥30; a = $\log_e$(attained age/60) and t = $\log_e$[(time since exposure)/25]. The sex-specific β, γ, η, δ, and φ are uncertain parameters where sex-specific β is assumed to have log-normal distributions for solid cancers and a four-parameter beta distribution for leukemia; γ, η, δ, and φ are assumed to have normal uncertainty distributions when not constant.

baseline and radiation-related excess risk. This approach allowed for survival probabilities to vary by sex, race/ethnicity, and age and to change over calendar time. Further details are found in Appendix B.

Calculation of excess and attributable fractions

The number of lifetime excess cancers for a given cancer type associated with age at exposure, e; attained age, a; latency period, l; transfer weight, w; and baseline cancer rate B(a) at attained age a is

$$\sum_{a=e+l}^{90} py(a)[w \times B(a) \times ERR + (1-w) \times EAR] \quad (2)$$

where py(a) is the person-years at risk of cancer during a single year age interval adjusted by the life table probability of survival to age a. The equation above is a simplified version for ease of exposition, since baseline cancer rates B(a) depend on age, sex, race/ethnicity, and calendar year, and as described previously, the ERR and EAR depend on age at exposure, attained age, sex, and tissue-specific dose. In the presentation of the results, we rounded excess numbers to the nearest multiple of 10, and we do not present any numbers <10 after rounding.

Values for baseline and excess numbers of cancer cases were converted to estimates of attributable fractions, i.e., the projected proportion of cancers attributable to radiation dose, by dividing the excess number of cancers by the total number, computed as the sum of baseline and excess cases. These estimates, which incorporate latency, attained age, and calendar time into person-years at risk, correspond to attributable fraction measures based on incidence density in a closed cohort (Greenland and Robins 1988).

Uncertainty

Our study accounts for many important but not all possible sources of uncertainty. We accounted for uncertainty in the baseline cancer rates, model parameters, model transfer weights, and radiation doses. For some sources, the uncertainty magnitudes were based on empirical data, while for others the magnitudes of uncertainty were obtained more subjectively from experts. The uncertainty of each component used in the calculation of the excess number of cancers was described using probability distribution functions. Parametric bootstrap methods were used to propagate these numerous sources of uncertainty. Possible sources of uncertainty not accounted for include census-based population information, national life tables, the extrapolation of model parameters to low doses and low dose rates, and changes in environmental and lifestyle factors that may have impacted the baseline cancer rates in early periods.

Since baseline cancer rates for the population of New Mexico were computed based on Poisson models for the periods 1945 to 1972 and 2016 to 2034, while we used SEER rates more directly for the periods 1972 to 2015, different approaches were implemented for accommodating uncertainty in the baseline rates depending on the calendar period. For years 1973 to 2015, we assumed the number

of cancer cases for a specific cancer site was distributed according to a Poisson distribution with the age- and sex-specific counts and standard deviations provided by the SEER program. Uncertainty for models extrapolating cancer risks from 1945 to 1972 and 2016 to 2034 used estimated parameters and covariance matrices describing the correlations between parameters from the fitted Poisson models in the baseline cancer risk models to generate rates directly from the Poisson models. See Appendix A for details.

The uncertainty in the ERR and EAR computations (eqn 1) arises from two different sources: the uncertainty in the parameters that are used and the uncertainty in the reconstructed dose. We accounted for uncertainty in model parameters used for ERR and EAR similarly to the BEIR VII report. The parameters in Table 3 were assumed to be random variables, with β_M and β_F arising from log-normal distributions for solid cancers and from four-parameter beta distributions for leukemia. Parameters γ, η, δ, and φ were assumed to have either normal distributions or were assumed to be constant when no uncertainty limits were provided. The β_M and β_F parameters for solid cancers in Table 3 were assumed to be medians or geometric means (with 95% uncertainty limits) and were converted to arithmetic means in the ERR and EAR calculations using the standard deviation calculated from the uncertainty distribution. For example, for colon cancer with β_M distributed log-normally with upper and lower uncertainty limits UL and LL, respectively, the mean for the parameter β_M was calculated as,

$$\beta_M \text{ mean} = \beta_M \exp\left(\frac{\left(\frac{LnUL - LnLL}{2 \times 1.96}\right)^2}{2}\right).$$

Total tissue-specific doses used in eqn (1) were assumed to be log-normally distributed (Simon et al. 2020).

An important component of uncertainty relates to the transfer of excess relative risk (multiplicative) and absolute (additive) risks to the 1945 New Mexico population from data derived largely from Japanese atomic bomb survivors. This uncertainty arises from the lack of knowledge about which type of risk projection is accurate. The estimated excess number of cases due to radiation exposure may be highly sensitive to the choice of weights, w, for the ERR and EAR (eqn 2). We took a conservative approach, similar to BEIR VII, in incorporating the uncertainty in the choice of weights by assuming the weight follows a Bernoulli distribution (NRC 2005). For example, for colon cancer, when the multiplicative transport weight was taken to be 0.7, the weight for the additive transport was $1-w = 0.3$, and the variance of the weight was 0.7×0.3. In contrast, only multiplicative projections were used for thyroid cancer and consequently, no uncertainty was assigned to w.

Dose uncertainty was also accounted for. An assessment of uncertainty found the uncertainty distribution on the best estimate of dose within a race/ethnicity and age group in a specified precinct to be log-normal (Simon et al. 2020). For the dose uncertainty component of the risk projection, we randomly drew a dose realization from a log-normal distribution that had as parameters the median dose (i.e., "best estimate") and the variance computed from the geometric standard deviation (by age, voting precinct, and race/ethnicity). To examine the impact of dose uncertainty on our 90% uncertainty intervals (UIs) for the number of excess cancer cases, we compared our results for the total population (years 1945–2034) to results that did not incorporate dose uncertainty (Appendix C).

Parametric bootstraps/dose simulations based on the assumptions described above generated 1,000 realizations of baseline and excess cases from which we calculated 1,000 realizations of attributable fractions for each of 721 voting precincts, 4 race/ethnicities, 90 exposure ages, male and females, 90 calendar years of follow-up, and 6 cancer groups. The estimated numbers of cancers were summed to obtain totals for the entire New Mexico population and population sub-groups defined by selected counties/other counties, and race/ethnicity categories. Using the 1,000 realizations of the projected number of excess cancers, medians, means, and 90% uncertainty intervals (based on the 5th and 95th percentiles of the bootstrap distribution for the respective quantity), and corresponding attributable fractions were then generated for each cancer type and selected sub-population. By providing medians, means, and 90% UIs, we intend to stress that our estimates should not be interpreted as precise numbers but rather as ranges of possible excess cancer cases and attributable fractions.

RESULTS

Our estimates of excess cancer cases assume 581,489 residents of New Mexico were alive at the time of the Trinity test in July 1945 (Table 1). After accounting for a 2-y latency period for leukemia and a 5-y latency period for solid cancers, we calculated a total of 26.6 million person-years at risk of leukemia and 24.9 million person-years at risk of solid cancers from 1945 until 2034 or age 90 y, which ever came first (Table 4).

The total lifetime baseline number of all solid cancers (excluding thyroid and NMSC) was estimated to be 183,000 from 1945 to 2034, which is approximately 31% of the population alive and residing in New Mexico at the time of the Trinity test (Table 4). We estimated a radiation excess 90% UI of 210 to 460 for solid cancers (except thyroid and NMSC) corresponding to an attributable fraction between 0.12% and 0.25% of all solid cancer cases in this population. We estimated an excess 90% UI of 80 to 530 thyroid cancer cases from 1945 to 2034, representing a range for the attributive fraction of 3.6% to 20% in the total population. The 1945

to 2015 period includes most of the baseline and excess cancers, which represents 0 to 70 y since the test and about 96% of the estimated person-years.

Estimated numbers of baseline cancers, radiation-related excess cancers, and the proportion of total cancer risk attributable to Trinity fallout are shown for selected counties in Table 4. Among the 30 counties in New Mexico at the time of the test, the counties of Guadalupe, Lincoln, San Miguel, Socorro, and Torrance had the highest attributable risk ranges of all solid cancer (except thyroid and NMSC) and accounted for over 70% of excess cancer cases. The 90% UIs of the total projected number of cancers in these counties were 150 to 330 for all solid cancers (except thyroid and NMSC), 60 to 370 for thyroid cancer, and up to 10 for leukemia (except CLL), with attributable fractions ranging from 0.65% to 1.4%, 17% to 58%, and 0.12% to 2.1%, respectively. The county-specific attributable risk 90% UIs of thyroid cancer are shown in Fig. 1.

Projected baseline and radiation-related cancers and proportion of total cancer risk attributable to radioactive fallout are shown by race/ethnicity in Table 5. The number of mean baseline and excess cancer cases was highest among Whites, primarily reflecting the population size of Whites at the time of the test. Whites contributed up to 14.9 million person-years to the time at risk, and we estimated an excess with an upper 90% uncertainty limit of <10 for leukemia (except CLL), 90% UIs 50 to 330 for thyroid cancer, and 130 to 310 for all solid cancers (except for thyroid and NMSC). These correspond to attributable fraction 90% UIs of 0.02% to 0.31%, 3.6% to 20%, and 0.11% to 0.26%, respectively. Hispanics contributed about 10 million person-years, and we estimated an excess 90% UIs of up to 10 for leukemia (except CLL), 30 to 210 for thyroid cancer, and 70 to 160 for all solid cancers (except for thyroid and NMSC). These corresponded to attributable fraction 90% UIs of 0.02% to 0.35%, 3.4% to 22%, and 0.13% to 0.29%, respectively. Native Americans contributed approximately 1.5 million person-years, and we estimated an excess number of cases with an upper 90% uncertainty limit of <10 thyroid cancers and <10 solid cancers (except for thyroid and NMSC), corresponding to attributable fraction 90% UIs of 0.63% to 4.2% and 0.03% to 0.07%, respectively. African Americans contributed up to 232,000 person-years, and we estimated an excess number of cases with an upper 90% uncertainty limit of <10 thyroid cancers and <10 all solid cancers (except for thyroid and NMSC) corresponding to attributable fraction 90% UIs of 0.83% to 5.5%, and 0.02% to 0.05%, respectively.

We compared the length of the 90% UIs for our results for the total population (years 1945–2034) to results that did not incorporate dose uncertainty. Not incorporating dose uncertainty substantially reduced the length of the 90% UIs by 25% for leukemia (except CLL), 31% for stomach cancer, 36% for colon cancer, 40% for all solid cancers (except thyroid cancer and NMSC), 49% for lung cancer, and 50% for thyroid cancer. The sources of uncertainty for the remainders of the 90% UI length included baseline cancer rates, transport model weighting, and BEIR VII radiation-related cancer risk parameters.

DISCUSSION

Despite the widespread interest in quantifying the cancer burden from Trinity through an observational epidemiological study, it was not feasible to conduct a study of that type in part because of the absence of a tumor registry in New Mexico in the 30 y immediately following the nuclear test. Instead, the current study uses newly estimated radiation doses and existing epidemiologically-based radiation risk data to estimate cancer risks to the radiation-exposed population of New Mexico. We applied estimates of tissue-specific radiation doses to the populations of 721 precincts of New Mexico by age and race/ethnicity to information from published, publicly available New Mexico census data, US life tables, US baseline cancer rates, and radiation risk model parameters derived primarily from study of the Japanese atomic bomb survivors.

In this work, we determined the five counties of Guadalupe, Lincoln, San Miguel, Socorro, and Torrance likely accounted for over two-thirds of excess cancers and reported the estimated excess and corresponding ranges for these counties combined (Table 4). Similarly, we reported the excess cancer for the other 25 counties combined. The distribution of attributable fractions for thyroid cancer shown by county (Fig. 1) reflects the dose estimation (Simon et al. 2020). In this work and that of Simon et al. (2020), both the organ doses and the resulting excess cancer cases were estimated at the voting precinct level and summed at the county level. While precincts in counties far outside the main fallout pattern (see Bouville et al. 2020, Fig. 1), were relatively homogenous in the exposures they received, the exposure levels in precincts in counties within the main fallout deposition pattern were much more heterogenous (Simon et al. 2020). In counties within the fallout pattern, the precise boundaries of the fallout deposition pattern relative to the precinct boundaries locations were difficult to assess. Consequently, precinct-level doses and cancer risks are not reported because such small divisions are not considered reliable.

Among single cancer sites, in the total population, county subgroups, and in all race/ethnicities represented in Tables 4 and 5, the fraction of cancer cases attributable to radiation exposure was highest for thyroid cancer. This reflects the large effect of exposure to the radioactive isotope ^{131}I in fallout from nuclear weapons tests. Iodine concentrates in the thyroid gland, which uses iodine to produce thyroid hormones, resulting in exposures generally much greater than
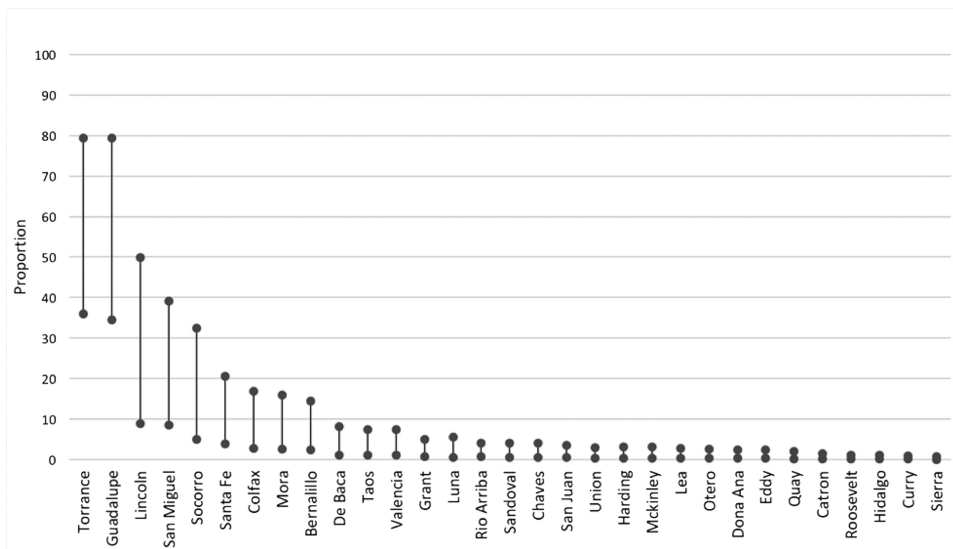
Table 4. Projected numbers of baseline cancers, excess radiation-related cancers, and proportion (in %) of total cancer risk attributable to radioactive fallout, by county group, cancer type, and time period (uncertainty distributions for excess cases represented by their means, medians, 5th and 95th percentiles). Abbreviations: PY, person-years. Results for person years, baseline, and excess presented for three significant digits or rounded to the 10th. Attributable risk presented for two significant digits or rounded to the hundredth.

| | | | Projected lifetime cancers, 1945–2034 | | | | | | | | | | | Estimated cancers, 1945–2015 | | | | | | | | | |
| | | | Excess cases | | | | Attributable risk (%) | | | | | | Excess cases | | | | Attributable risk (%) | | | |
Group/Cancer	PY	Baseline	5%	Median	Mean	95%	5%	Median	Mean	95%	PY	Baseline	5%	Median	Mean	95%	5%	Median	Mean	95%
Total																				
Leukemia[a]	26,600,000	2,900	<10	<10	<10	<10	0.02	0.09	0.12	0.31	25,500,000	2,580	<10	<10	<10	<10	0.02	0.1	0.13	0.34
Thyroid	24,900,000	2,170	80	210	240	530	3.6	8.7	9.7	20	23,800,000	1,880	60	150	180	380	3.1	7.5	8.4	17
Colon	24,900,000	16,300	20	30	30	40	0.11	0.17	0.17	0.25	23,800,000	14,600	20	20	20	40	0.1	0.15	0.16	0.24
Stomach	24,900,000	5,180	<10	<10	<10	20	0.02	0.03	0.1	0.33	23,800,000	4,650	<10	<10	<10	10	0.02	0.03	0.09	0.29
Lung	24,900,000	26,500	20	30	40	60	0.07	0.12	0.14	0.23	23,800,000	23,700	10	20	30	50	0.06	0.1	0.11	0.21
All Solid[b]	24,900,000	183,000	210	310	320	460	0.12	0.17	0.17	0.25	23,800,000	160,000	170	250	260	370	0.11	0.16	0.16	0.23
Selected counties[c]																				
Leukemia[a]	3,210,000	360	<10	<10	<10	<10	0.12	0.62	0.82	2.1	3,070,000	320	<10	<10	<10	<10	0.13	0.67	0.88	2.3
Thyroid	3,010,000	270	60	150	170	370	17	35	36	58	2,870,000	230	40	110	130	270	15	32	33	54
Colon	3,010,000	1,970	10	20	20	30	0.66	0.97	1.0	1.5	2,870,000	1,760	10	20	20	30	0.59	0.89	0.94	1.4
Stomach	3,010,000	620	<10	<10	<10	20	0.13	0.21	0.75	2.4	2,870,000	550	<10	<10	<10	10	0.12	0.20	0.67	2.1
Lung	3,010,000	3,230	20	30	30	60	0.56	0.95	1.0	1.8	2,870,000	2,880	10	20	30	50	0.43	0.73	0.87	1.6
All Solid[b]	3,010,000	22,400	150	210	220	330	0.65	0.94	0.98	1.4	2,870,000	19,600	120	180	180	270	0.61	0.89	0.92	1.3
Other counties																				
Leukemia[a]	23,400,000	2,540	<10	<10	<10	<10	0	0.02	0.02	0.06	22,500,000	2,260	<10	<10	<10	<10	0	0.02	0.02	0.06
Thyroid	21,900,000	1,900	20	60	70	150	1.2	3.0	3.6	7.4	21,000,000	1,650	20	40	50	110	1.1	2.6	3.0	6.3
Colon	21,900,000	14,400	<10	<10	<10	10	0.04	0.06	0.06	0.08	21,000,000	12,900	<10	<10	<10	10	0.03	0.05	0.05	0.08
Stomach	21,900,000	4,560	<10	<10	<10	<10	0	0	0.02	0.05	21,000,000	4,100	<10	<10	<10	<10	0	0	0.01	0.05
Lung	21,900,000	23,300	<10	<10	<10	<10	0.01	0.01	0.01	0.02	21,000,000	20,900	<10	<10	<10	<10	0	0.01	0.01	0.02
All Solid[b]	21,900,000	160,000	60	90	90	130	0.04	0.06	0.06	0.08	21,000,000	141,000	50	70	80	110	0.04	0.05	0.05	0.08

[a] Excludes CLL (chronic lymphocytic leukemia).

[b] All solid cancers except thyroid and non-melanoma skin cancer.

[c] Selected counties include five counties with the highest attributable risk of all solid cancer: Guadalupe, Lincoln, San Miguel, Socorro, and Torrance.

Fig. 1. Uncertainty intervals (5%, 95%) for proportion (in %) of thyroid cancer risk attributable to radioactive fallout from the Trinity nuclear test by county among New Mexico residents alive in 1945 (1945 to 2034).

for other organs of the body. The radioactive isotope ^{131}I is indistinguishable by the thyroid gland from the non-radioactive version, making the thyroid gland especially vulnerable to this form of radiation, particularly during childhood, as has been reported in population-based studies of Chernobyl fallout (Brenner et al. 2011; Zablotska et al. 2011). The estimates for attributable fraction of thyroid cancer were highest for Hispanics and Whites, reflecting higher intakes of dairy products and locations of residence for these groups. However, the uncertainty around these estimates was substantial, and 90% uncertainty intervals for attributable fractions of thyroid cancer do not support strong differences across races/ethnicities.

There are several limitations that must be considered in the interpretation of our excess and attributable fractions estimates. While the association between ionizing radiation and cancer risk is considered one of the best quantified dose-response relationships for any environmental agent, the estimated number of excess cases is still uncertain and depends on numerous assumptions and input data. In this work, we sought to use the best available published data as input to our calculations and to make assumptions that would not knowingly or purposefully bias the estimates.

The study population and distribution of race/ethnicity was estimated based on US census data from 1940 and 1950 as that was the government-documented data available to this study (USCB 2019). However, use of census data is acknowledged to have possibly resulted in underestimates of the numbers of certain groups if they were less likely to participate in the census for either year. This could have been the case, for example, for Native Americans who, through 1950, were racially identified by a census taker rather than the individual interviewed (Jobe 2004). Hispanics were identified by those self-reporting the "Spanish mother tongue," which may have underestimated the proportion of the New Mexico

population in that race/ethnicity category. Similarly, national life tables were used that for many years correspond to data collected by the United States Census Bureau and may not have accurately described the experience of all ethnic and racial groups in New Mexico. In addition, possible nonlinear changes, e.g., those caused by World War II, in the population distribution during the period of time between the two censuses were not accounted for.

Cancer incidence data were not systematically collected for residents of New Mexico for the entire time period (Gibson and Jung 2002) in our study, so we relied on available data from high quality cancer registries in the United States SEER program that started in 1973 and have been updated until 2015 to obtain stable estimates of age-, sex-, and race/ethnicity-specific baseline cancer rates, projecting rates for periods 1945–1972 and 2016–2034, which were outside the time period captured by SEER. We limited the scope of projection to ages under 90 y and calendar year before 2034, for which projections of baseline cancer rates are more reliable. Projected baseline cancer rates prior to 1973 did not account for changes in environmental and lifestyle risk factors. For example, the broader availability of refrigeration in the 1940s, which reduced helicobacter pylori prevalence, possibly results in an underestimation of stomach cancer incidence in the early period (Luo et al. 2017). Modeled racial and ethnic patterns for cancer incidence based on data obtained from the SEER program do reflect racial and ethnic patterns in cancer mortality that have been reported for New Mexico from 1958 to 1982 (Becker et al. 1993). For example, similarly to Becker and colleagues, we estimated a near two-fold increased risk of stomach cancer among Hispanics compared to Whites. Overall, cancer incidence for residents of New Mexico has been reported to be lower than the entire United States (NCI 2019), which

Table 5. Projected numbers of baseline cancers, excess radiation-related cancers, and proportion (in %) of total cancer risk attributable to radioactive fallout, by race/ethnicity, cancer type, and time period (uncertainty distributions for excess cases represented by their means, medians, 5th, and 95th percentiles). Abbreviations: PY, person-years. Results for person years, baseline, and excess presented for three significant digits or rounded to the 10th. Attributable risk presented for two significant digits or rounded to the hundredth.

| | | | Projected lifetime cancers, 1945–2034 | | | | | | | | | Estimated cancers, 1945–2015 | | | | | | | | | |
| | | | Excess cases | | | | Attributable risk (%) | | | | | | Excess cases | | | | Attributable risk (%) | | | |
Race/Cancer	PY	Baseline	5%	Median	Mean	95%	5%	Median	Mean	95%	PY	Baseline	5%	Median	Mean	95%	5%	Median	Mean	95%
Whites																				
Leukemia[a]	14,900,000	1,720	<10	<10	<10	<10	0.02	0.09	0.12	0.31	14,300,000	1,510	<10	<10	<10	<10	0.02	0.1	0.13	0.34
Thyroid	13,900,000	1,310	50	130	150	330	3.6	8.9	9.9	20	13,300,000	1,130	40	90	110	240	3.1	7.6	8.5	17
Colon	13,900,000	10,400	10	20	20	30	0.11	0.17	0.17	0.26	13,300,000	9,440	<10	10	20	20	0.1	0.15	0.16	0.25
Stomach	13,900,000	2,120	<10	<10	<10	10	0.02	0.03	0.15	0.49	13,300,000	1,910	<10	<10	<10	<10	0.02	0.03	0.13	0.43
Lung	13,900,000	19,200	10	20	20	50	0.06	0.11	0.13	0.24	13,300,000	17,100	<10	10	20	40	0.05	0.08	0.11	0.23
All Solid[b]	13,900,000	119,000	130	200	200	310	0.11	0.16	0.17	0.26	13,300,000	105,000	100	160	170	250	0.1	0.15	0.16	0.24
Hispanics																				
Leukemia[a]	9,960,000	1,060	<10	<10	<10	<10	0.02	0.1	0.14	0.36	9,540,000	960	<10	<10	<10	<10	0.02	0.11	0.15	0.39
Thyroid	9,300,000	770	30	80	90	210	3.5	8.9	10	22	8,880,000	670	20	60	70	150	3.1	7.7	8.9	19
Colon	9,300,000	5,000	<10	10	10	20	0.13	0.2	0.2	0.3	8,880,000	4,310	<10	<10	<10	10	0.12	0.18	0.18	0.27
Stomach	9,300,000	2,680	<10	<10	<10	<10	0.02	0.03	0.09	0.26	8,880,000	2,390	0	0	0	<10	0.02	0.03	0.08	0.23
Lung	9,300,000	5,920	<10	10	10	20	0.12	0.18	0.2	0.31	8,880,000	5,310	<10	<10	<10	10	0.09	0.14	0.16	0.26
All Solid[b]	9,300,000	55,500	70	110	110	160	0.13	0.19	0.2	0.29	8,880,000	48,000	60	90	90	130	0.12	0.18	0.18	0.26
Native Americans																				
Leukemia[a]	1,570,000	100	<10	<10	<10	<10	0	0.01	0.02	0.04	1,500,000	90	<10	<10	<10	<10	0	0.01	0.02	0.04
Thyroid	1,470,000	80	<10	<10	<10	<10	0.63	1.6	1.9	4.2	1,400,000	70	<10	<10	<10	<10	0.56	1.4	1.7	3.7
Colon	1,470,000	760	<10	<10	<10	<10	0.02	0.04	0.04	0.06	1,400,000	670	<10	<10	<10	<10	0.02	0.03	0.03	0.05
Stomach	1,470,000	310	<10	<10	<10	<10	0	0	0.01	0.03	1,400,000	280	<10	<10	<10	<10	0	0	0.01	0.03
Lung	1,470,000	1,060	<10	<10	<10	<10	0	0.01	0.01	0.01	1,400,000	950	<10	<10	<10	<10	0	0	0	0.01
All Solid[b]	1,470,000	6,460	<10	<10	<10	<10	0.03	0.04	0.04	0.07	1,400,000	5,630	<10	<10	<10	<10	0.02	0.04	0.04	0.06
African Americans																				
Leukemia[a]	232,000	20	<10	<10	<10	<10	0	0.01	0.02	0.04	227,000	20	<10	<10	<10	<10	0	0.01	0.02	0.04
Thyroid	215,000	10	<10	<10	<10	<10	0.83	2.2	2.5	5.5	210,000	<10	<10	<10	<10	<10	0.74	1.9	2.2	4.7
Colon	215,000	210	<10	<10	<10	<10	0.02	0.03	0.03	0.06	210,000	200	<10	<10	<10	<10	0.02	0.03	0.03	0.05
Stomach	215,000	70	<10	<10	<10	<10	0	0	0.01	0.02	210,000	70	<10	<10	<10	<10	0	0	0.01	0.02
Lung	215,000	350	<10	<10	<10	<10	0	0	0	0.01	210,000	330	<10	<10	<10	<10	0	0	0	0.01
All Solid[b]	215,000	1,870	<10	<10	<10	<10	0.02	0.04	0.04	0.05	210,000	1,750	<10	<10	<10	<10	0.02	0.03	0.03	0.05

[a]Excludes CLL (chronic lymphocytic leukemia).

[b]All solid cancers except thyroid and non-melanoma skin cancer.

would imply that the number of estimated baseline and excess cancers may be overestimated under the multiplicative transfer model. However, inaccuracy in baseline cancer rates and all-cause mortality derived from US life tables apply similarly to estimates of excess and baseline cases, so that the projected proportion of cancer risk attributable to radioactive fallout, calculated as excess cases divided by the sum of baseline and excess cases, should not be appreciably impacted. Thus, we do not believe that these various limitations have substantially biased our estimates of attributable fractions presented in Tables 4 and 5 and Fig. 1.

Uncertainty in dose estimation is an important limitation of this study. Dose estimates were based on the fallout pattern, information collected about individuals' diet and lifestyle, and exposure models used to estimate doses for external and internal exposure from consumption of food, water, in-cloud inhalation, and resuspension over the first year following Trinity. Information on diet and lifestyle obtained from focus groups have inherent limitations, including memory recall and difficulty in sampling groups representative of all ages at the time of potential exposure. An analysis of dose uncertainty, based on Monte Carlo simulations using subjectively and experience-derived probability density functions resulted in geometric standard deviations on dose estimates ranging from 2.7 to 5.6 (Simon et al. 2020). When we compared our estimates of numbers of excess cancer cases for the total population (years 1945–2034) to those that did not incorporate dose uncertainty, we found that 25% to 50% of the length of the 90% uncertainty intervals could be attributed to dose uncertainty. Thus, uncertainty in dose estimation had a substantial impact on the total uncertainty around our estimates.

Excess relative and absolute risk models rely on evidence from Japanese atomic bomb survivors, many of whom were exposed to moderate to high doses and high dose rates that resulted from near-instantaneous prompt gamma ray exposure and very little protracted exposure from radioactive fallout. In contrast, the residents of New Mexico were potentially exposed to lower doses and low dose rates over a longer time since no New Mexico residents were close enough to the detonation to be exposed to prompt gamma rays (Simon et al. 2020). A DDREF of 1.5 was used in BEIR VII to extrapolate from populations with high-dose/high-dose rates to those with low-dose/low-dose rates, effectively reducing the number of estimated excess cancer cases. An evaluation of uncertainty in the BEIR VII report (Table 12-10, page 284), indicated that the main contribution to uncertainty for all solid cancers (except thyroid and NMSC) was the DDREF. The current analysis differs from the BEIR VII report in that we did not apply either a DDREF or incorporate uncertainty around the values for the DDREF. There continues to be substantial debate among experts as to how to best extrapolate to low doses (Ruhm et al. 2015; Rühm 2016; Shore et al. 2017; Tran and Little 2017). While the International Commission on Radiological Protection (ICRP) has proposed a DDREF of 2 (Wrixon 2008), the expert panel at the World Health Organization more recently did not apply a DDREF (i.e., they set DDREF equal to 1) to its health risk assessment following the nuclear accident in Fukushima (WHO 2013). In addition, recently updated and expanded pooled analyses of thyroid cancer, the organ most exposed to Trinity fallout, supports linearity of the dose-response in the low dose range (<0.2 Gy) (Veiga et al. 2016; Lubin et al. 2017).

Several other issues merit discussion. We did not account for uncertainty in the life table- and census-based estimates of person years at risk by age and race/ethnicity. It should also be restated that the doses captured exposure from only the first year after the detonation, corresponding to an estimated 90% of the lifetime dose. The effect of capturing 90% of the dose would suggest our risk projection might slightly underestimate total excess cases and attributable risk, particularly for cancer outcomes related to longer-lived radionuclides. We also did not project risk for the in utero exposed population, which may also lead to a slight underestimation of total excess cancer cases. Although dose estimates were available for this group, robust long-term epidemiological data are not available from which to obtain radiation-related risk parameters.

CONCLUSION

We provide estimates of the ranges of excess cancer cases from exposure to Trinity fallout to residents of New Mexico alive in 1945. In this analysis, we accounted for uncertainty of estimated doses, baseline cancer risks, model weights, and radiation-risk model parameters. There are several key conclusions from this analysis. Our 90% UIs suggest that as many as 1,000 or as few as 290 cancers have already occurred or are projected to occur in the future that would not have occurred in the absence of residential radiation exposure from Trinity fallout. Most of the excess cancers are projected to have occurred or will occur among residents of Guadalupe, Lincoln, San Miguel, Socorro, and Torrance counties in 1945. Uncertainty in dose estimation had a substantial impact in the total uncertainty around our estimates. Finally, most cancers that have occurred or will occur among the residents of New Mexico in 1945 are likely to be cancers unrelated to exposures from Trinity fallout.

to providing the data needed for this work. We thank William Wheeler from IMS for computing help. This work utilized the computational resources of the NIH HPC Biowulf cluster (http://hpc.nih.gov).

REFERENCES

Becker TM, Wiggins CL, Elliott RA, Key CR, Samet JM. Racial and ethnic patterns of mortality in New Mexico. Albuquerque: University of New Mexico Press; 1993.

Berrington de Gonzalez A, Iulian Apostoaei A, Veiga LH, Rajaraman P, Thomas BA, Owen Hoffman F, Gilbert E, Land C. Radrat: a radiation risk assessment tool for lifetime cancer risk projection. J Radiol Protect 32:205–222; 2012.

Bouville A, Beck HL, Thiessen KM, Hoffman FO, Potischman N, Simon SL. The methodology used to assess doses from the first nuclear weapons test (Trinity) to the populations of New Mexico. Health Phys 119:400–427; 2020.

Brenner AV, Tronko MD, Hatch M, Bogdanova TI, Oliynik VA, Lubin JH, Zablotska LB, Tereschenko VP, McConnell RJ, Zamotaeva GA, O'Kane P, Bouville AC, Chaykovskaya LV, Greenebaum E, Paster IP, Shpak VM, Ron E. I-131 dose response for incident thyroid cancers in Ukraine related to the Chornobyl accident. Environmental Health Perspectives 119:933–939; 2011.

CDC. United States lifetables [online]. Available at: ***https://www.cdc.gov/nchs/products/life_tables.htm***. Accessed 26 April 2019.

Gibson C, Jung K. Historical census statistics on population totals by race (1790 to 1990) and by hispanic origin (1970 to 1990) for large cities and urban places. Washington, DC: US Census Bureau; 2002.

Greenland S, Robins JM. Conceptual problems in the definition and interpretation of attributable fractions. Am J Epidemiol 128:1185–1197; 1988.

Hoffman JG. Nuclear explosion 16 July 1945, part c: transcript of radiation monitor's field notes. Film badge data on town monitoring. Los Alamos, NM: Los Alamos Scientific Laboratory; Nuclear Testing Archive, Las Vegas, Nevada, accession #NV0059839; 1945.

Jobe MM. Native Americans and the U.S. Census: a brief historical survey. Boulder, CO: University Libraries Faculty & Staff Contributions 28; 2004.

Land CE, Bouville A, Apostoaei I, Simon SL. Projected lifetime cancer risks from exposure to regional radioactive fallout in the Marshall Islands. Health Phys 99:201–215; 2010.

Lubin JH, Adams MJ, Shore R, Holmberg E, Schneider AB, Hawkins MM, Robison LL, Inskip PD, Lundell M, Johansson R, Kleinerman RA, de Vathaire F, Damber L, Sadetzki S, Tucker M, Sakata R, Veiga LHS. Thyroid cancer following childhood low-dose radiation exposure: a pooled analysis of nine cohorts. J Clin Endocrinol Metab 102:2575–2583; 2017.

Luo G, Zhang Y, Guo P, Wang L, Huang Y, Li K. Global patterns and trends in stomach cancer incidence: age, period and birth cohort analysis. Int J Cancer 141:1333–1344; 2017.

NCI. Quick profiles: New Mexico. [online] https://statecancerprofiles. cancer.gov. Accessed 26 April 2019. 2019.

NRC. Health risks from exposure to low levels of ionizing radiation: BEIR VII phase 2. Washington, DC: National Research Council (NRC) and Committee to Assess Health Risks from Exposure to Low Levels of Ionizing Radiation; 2005.

Potischman N, Salazar SI, Scott MA, Naranjo M, Hazous E, Bouville A, Simon SL. Methods and findings on diet and lifestyle used to support estimation of radiation doses from radioactive fallout from the Trinity nuclear test. Health Phys 119: 390–399; 2020.

Preston DL, Ron E, Tokuoka S, Funamoto S, Nishi N, Soda M, Mabuchi K, Kodama K. Solid cancer incidence in atomic bomb survivors: 1958-1998. Radiat Res 168:1–64; 2007.

Ron E, Lubin JH, Shore RE, Mabuchi K, Modan B, Pottern LM, Schneider AB, Tucker MA, Boice JD Jr. Thyroid cancer after exposure to external radiation: a pooled analysis of seven studies. Radiat Res 141:259–277; 1995.

Rühm W. Dose-rate effects in radiation biology and radiation protection. Washington, DC: ICRP; 2016.

Rühm W, Woloschak GE, Shore RE, Azizova TV, Grosche B, Niwa O, Akiba S, Ono T, Suzuki K, Iwasaki T, Ban N, Kai M, Clement CH, Bouffler S, Toma H, Hamada N. Dose and dose-rate effects of ionizing radiation: a discussion in the light of radiological protection. Radiat Environ Biophys 54:379–401; 2015.

Rühm W, Azizova TV, Bouffler SD, Little MP, Shore RE, Walsh L, Woloschak GE. Dose-rate effects in radiation biology and radiation protection. Ann ICRP Jun;45(1 suppl):262–279; 2016. doi: 10.1177/0146645316629336.

SEER 13: Surveillance, Epidemiology, and End Results (SEER) Program (www.seer.cancer.gov) SEER*Stat Database: Incidence - SEER 13 Regs Research Data, Nov 2017 Sub (1992-2015) <Katrina/Rita Population Adjustment> - Linked To County Attributes - Total U.S., 1969-2016 Counties, National Cancer Institute, DCCPS, Surveillance Research Program, released April 2018, based on the November 2017 submission. Accessed 27 February 2019.

SEER 18: Surveillance, Epidemiology, and End Results (SEER) Program (www.seer.cancer.gov) SEER*Stat Database: Incidence - SEER 18 Regs Research Data + Hurricane Katrina Impacted Louisiana Cases, Nov 2017 Sub (2000-2015) <Katrina/Rita Population Adjustment> - Linked To County Attributes - Total U.S., 1969-2016 Counties, National Cancer Institute, DCCPS, Surveillance Research Program, released April 2018, based on the November 2017 submission. Accessed 27 February 2019.

SEER 18: Surveillance, Epidemiology, and End Results (SEER) Program (www.seer.cancer.gov) SEER*Stat Database: Incidence - SEER 18 Regs Research Data + Hurricane Katrina Impacted Louisiana Cases, Nov 2017 Sub (2000-2015) <Katrina/Rita Population Adjustment> - Linked To County Attributes - Total U.S., 1969-2016 Counties, National Cancer Institute, DCCPS, Surveillance Research Program, released April 2018, based on the November 2017 submission. Accessed 27 February 2019.

Shore R, Walsh L, Azizova T, Ruhm W. Risk of solid cancer in low dose-rate radiation epidemiological studies and the dose-rate effectiveness factor. Int J Radiat Biol 93:1064–1078; 2017.

Simon SL, Bouville A, Beck HL, Melo DR. Estimated radiation doses received by New Mexico residents from the 1945 Trinity nuclear test. Health Phys 119:428–477; 2020.

Tran V, Little MP. Dose and dose rate extrapolation factors for malignant and non-malignant health endpoints after exposure to gamma and neutron radiation. Radiat Environ Biophys 56: 299–328; 2017.

USCB. Census of population and housing [online]. 2019. Available at: ***https://www.census.gov/prod/www/decennial.html***. Accessed 13 May 2019.

Veiga LH, Holmberg E, Anderson H, Pottern L, Sadetzki S, Adams MJ, Sakata R, Schneider AB, Inskip P, Bhatti P, Johansson R, Neta G, Shore R, de Vathaire F, Damber L, Kleinerman R, Hawkins MM, Tucker M, Lundell M, Lubin JH. Thyroid cancer after childhood exposure to external radiation: an updated pooled analysis of 12 studies. Radiat Res 185:473–484; 2016.

WHO. Health risk assessment from the nuclear accident after the 2011 Great East Japan earthquake and tsunami based on a preliminary dose estimation. Geneva: World Health Organization; 2013.

Wrixon AD. New recommendations from the international commission on radiological protection—a review. Phys Med Biol 53:R41–60; 2008.

Zablotska LB, Ron E, Rozhko AV, Hatch M, Polyanskaya ON, Brenner AV, Lubin J, Romanov GN, McConnell RJ, O'Kane P, Evseenko VV, Drozdovitch VV, Luckyanov N, Minenko VF, Bouville A, Masyakin VB. Thyroid cancer risk in Belarus among children and adolescents exposed to radioiodine after the Chornobyl accident. Br J Cancer 104:181–187; 2011.

APPENDIX A: BASELINE CANCER RATES

Cancer incidence rates for the full period 1945 to 2034 were estimated by age at diagnosis, calendar year, sex, and race/ethnicity using data reported by the Surveillance, Epidemiology, and End Results (SEER) cancer registry program from 1973 to 2015. Since the SEER registries contained Hispanic ethnicity-specific data beginning in 1992, the period following 1992 was used to calculate race/ethnicity rate ratios that were applied to earlier periods. All solid cancers included ICDO-III codes C00-C89 behavior 3, excluding leukemia, lymphoma, myeloma, and other lympho-hematopoietic malignancies, plus brain and CNS tumors of benign, uncertain, or unknown behavior (ICDO-III codes C70-C72, behavior 0,1) with in situ excluded. Site-specific codes were C34 for lung, C18 for colon, C16 for stomach, and C73 for thyroid. For leukemia, all malignant leukemia was included except CLL based on the ICD-O-3/WHO 2008 definition (SEER 2019). Fig. A1 shows an example of the baseline cancer estimation by calendar year for all cancer groups, by race/ethnicity, males and females, for the 80–84-y age group.

Years 1945 to 1972

We used rates for all races/ethnicities combined from 1973 to 1987 from SEER 9 to extrapolate rates from 1945 to 1972 (Rühm et al. 2016). We modeled 5-y age-specific rates for all cancers. As there were very few cancers observed in the 0–4-y age groups, we combined that group with the 5–9-y age group and used 17 age groups in the modeling for thyroid cancer, leukemia (except CLL), and all solid cancers (excluding thyroid and NMSC) combined. We fit Poisson regression models that included the age groups coded with dummies, calendar year in single years treated as a continuous variable fitted with a linear trend, sex and interaction terms of year by sex, and age groups by sex (17 degrees of freedom). For colon, lung and stomach cancer, we combined the 0–4, 5–9, and 10–14 y age groups into a single 15-y category and used 16 age categories. The terms in the Poisson model were the same otherwise (interaction of sex by age group, year, interaction of sex by year).

Race/ethnicity ratios using SEER rates for each site were computed using data from 1992 to 2006. We fit Poisson models to race/ethnicity specific counts and populations SEER 9 rates, adjusted for race/ethnicity [all race/ethnicities combined (ALL), Black, Non-hispanic White, Native American, Hispanics], age (trend, single years), and calendar year (single years, treated as a continuous variable) with "ALL" as the reference group. We then tested if there were year by race interactions in the Poisson models. There were some minor deviations from a constant race/ethnicity ratio by year for the following sites/races/ethnicities: Hispanics for colon (men and women) and White women for stomach, which we did not accommodate further as they were not significant after controlling for multiple testing. The extrapolated rates from 1945 to 1972 were multiplied by the race/ethnicity ratio to obtain race/ethnicity and age-specific rates for each cancer site. The same race/ethnicity ratios were also applied to cancer rates for all races combined from SEER 9, from 1972 to 1992, as not all race/ethnic groups were available in SEER during that period. For lung and all solid cancers, the race/ethnicity ratio estimates differed by sex; for all other sites, they were the same for men and women.

Years 1973 to 1991

The same race/ethnicity ratios used for the 1945 to 1972 period were also applied to cancer rates for all races/ethnicities combined from SEER 9, from 1973 to 1992, as not all race/ethnic groups were available in SEER during that time period.

Years 1992 to 2015

To use the most comprehensive data available in SEER, incidence rates by age at diagnosis, calendar year, sex, and race/ethnicity used SEER 13 from 1992–1999 and SEER 18 from 2000–2015 (SEER13 2018, SEER18 2018).

Years 2016 to 2034

To obtain cancer rates for projections from 2016 to 2034 (inclusive), we used sex- and race/ethnicity-specific rates from SEER18, 2000 to 2015 (SEER18 2018). We fit Poisson models including age in 5-y groups coded with dummies, calendar year in single years (centered at 2007), sex, and race/ethnicity and included interaction terms of race/ethnicity with year, age, and sex for all sites. For all solid cancers, we fit separate models for men and women that otherwise had the same parametrization. Calendar year was fit with a linear trend (which seemed appropriate after some model checking). The coefficients from the Poisson models were then used to project the rates.

APPENDIX B: LIFETABLES

Availability of published US lifetables varied by calendar year and race/ethnicity. Separate male and female survival probabilities were available for each year and race/ethnicity in the table. We allowed for changes in survival probability across calendar years by updating the lifetables every decade, which represented the period in which they became available. Race/ethnicity-specific lifetables were not available for non-Whites until 1999. When a specific race/ethnicity was not available,

Table B1. Selection of life tables by race/ethnicity for years 1945 to 2034.

Years	Lifetable years	Race/ethnicity			
		White	Hispanic	African American (AA)	Native American
1945–1948	1939-41	White	White	White	White
1949–1958	1949-51	All races	All races	All races	All races
1959–1968	1959-61	White	Non-white	Non-white	Non-white
1969–1978	1969-71	White	Non-white	Non-white	Non-white
1979–1988	1979-81	White	Non-white	Non-white	Non-white
1989–1998	1989-91	White	Non-white	Non-white	Non-white
1999–2008	1999-01	White	All races	AA	All races
2009–2015	2009	White	Hispanic	AA	All races
2016–2034	2015	White	Hispanic	AA	All races

we used lifetables for either non-Whites, all races, or what was available. For example, a lifetable based on data from 1939 to 1941 among Whites was used for each race/ethnicity for the period 1945 to 1948. Table B1 summarizes the lifetables we used to estimate survival probability by calendar period and race/ethnicity.

APPENDIX C: BOOTSTRAP VARIANCE COMPUTATION

We computed the variance of the following quantity,

$$O = \sum_{i=1}^{K} personyears(i)*$$

$$[B(i)*ERR(i)*raceratio*w + (1-w)*EAR(i)],$$
$$(C1)$$

where *personyears(i)* was the observed number of person-years in a cell defined by precinct, sex, age, race, and calendar year using a bootstrap procedure; *w* was the transfer weight; *raceratio*, the ratio of cancer incidence rates for different race/ethnicities; *B(i)* is the baseline cancer rates per cell; *ERR(i)* is the excess relative risk per cell; and *EAR(i)* is the excess absolute risk per cell. We assumed that the person-years were fixed, as their variability is expected to be small compared to the variability in the baseline rates, the race/ethnicity ratio (when incorporated) and the *ERR* and *EAR* functions.

The variance computation for the baseline counts that only used baseline rates, but not the *EAR* and *ERR* functions, proceeded along the same lines. Once we obtained 1,000 bootstrap values of *O*, the 90% confidence interval around the original estimate was calculated by taking the 5th and 95th percentile of the bootstrap empirical distribution function as the lower and upper confidence limit, respectively. Details for the individual component of eqn (C1) follow next.

Bootstrap for the baseline rates

The bootstrap computation for the baseline rates differed by calendar time period. For the 1945 to 1972 and 2016–2034 periods, we used a parametric bootstrap to account for the uncertainty in the predicted rates. We resampled coefficients for each of the Poisson models from a multivariate normal distribution that had as the mean the parameter estimates and the covariance matrix as estimated from the original model fit to the SEER data. Similarly, we assumed that the estimates of the race/ethnicity ratio parameters arose from a normal distribution with known mean and covariance, and resampled values from a multivariate normal distribution with that mean and covariance matrix. These new estimates were used in the computation of the rates and the observed and excess numbers of cancers.

For the 1972 to 1991 period, we used SEER rates for the baseline rates, which we multiplied by a race/ethnicity ratio to obtain race/ethnicity specific rates. We thus obtained bootstrap counts in cell *I* by resampling counts from a Poisson distribution that has the mean the number of cases in cell *i* reported in SEER, with the person years observed in that cell. The race/ethnicity ratio uncertainty was again incorporated by sampling the corresponding parameters as described for the 1945 to 1972 period.

For the 1992 to 2015 period, the age, sex, and race/ethnicity specific rates were directly obtained from SEER, and we resampled counts from a Poisson distribution, as described for the 1972 to 1991 period, without any further race/ethnicity adjustment.

Bootstrap for ERR and EAR

The uncertainty in the ERR and EAR computations came from two different sources: the uncertainty in the parameters that are used, and the uncertainty in the reconstructed dose. We used a parametric bootstrap to incorporate uncertainty around parameter values in the ERR and EAR functions, given by eqn (1) (rewritten below for convenience),

$$ERR(D, s, e, a, t) \ or \ EAR(D, s, e, t)$$

$$= \beta_s D exp(\gamma e + \eta a + \delta t + \varphi et),$$

where $D = dose$ is in Gy, $e =$ (exposure age-30)/10 for exposure age<30 and $e = 0$ for exposure age $\geq$ 30, $a = \log_e$ (attained age/60) and $t = \log_e$(time since exposure/25) where time since exposure is attained age minus age at exposure.

We used distributional assumptions based on recommendations in the BEIR VII report (NRC 2005). For normally (or log-normally) distributed parameters, we resampled values from a normal distribution that had as the true parameter values the mean and variances given in the BEIR VII report. We assumed that parameters β_M and β_F in the ERR and EAR models followed a log-normal distribution for every site except leukemia for which we sampled values from the normal

distribution with the appropriate mean and variance and then exponentiated them. For leukemia, the β_M and β_F parameters were assumed to arise from a four-parameter beta distribution. We thus first applied the inverse normal density to them, and then the cumulative distribution function of a four-parameter beta distribution. The parameters for the four–parameter beta distribution were obtained by solving a set of linear equations in the published confidence bounds and the mean, knowing that the lower interval bound was zero, to match up the intervals given in BEIR VII (NRC 2005).

For leukemia and all solid cancers, we additionally incorporated the covariance between the parameter values. First, we drew all parameters for a multivariate normal distribution and then exponentiated the first two components for all solid cancers. Note that the covariances are not preserved after exponentiating.

For all solid cancers, $\delta = 0$ and $\varphi = 0$ in eqn (1) for ERR. The remaining ERR parameters have means $\log_e(\beta_M) = -1.104$; $\log_e(\beta_F) = -0.558$; $\gamma = -0.3$; $\eta = -1.4$. For the EAR function for all solid cancers, $\delta = 0$ and $\varphi = 0$ in eqn (1) and the remaining ERR parameters have means $\log_e(\beta_M) = -6.1$; $\log_e(\beta_F) = -5.876$; $\gamma = 2.779$; $\eta = -0.4058$. The covariance matrices for the parameters in the ERR and EAR functions were

CovERR($\log_e(\beta_M)$, $\log_e(\beta_F)$ η γ) = [0.031703	0.010922	0.011666	
−0.021094			
0.010922	0.017866	0.0094576	
−0.011821			
0.011666	0.0094576	0.010547	
−0.023224			
−0.021094	−0.011821	−0.023224	0.14091];
CovEAR($\log_e(\beta_M)$, $\log_e(\beta_F)$ η γ) = [0.029955	0.0094495	0.0093699	
−0.0085991			
0.0094495	0.015269	0.0086235	
−0.015065			
0.0093699	0.0086235	0.0093004	
−0.020365			
−0.0085991	−0.015065	−0.020365	0.10435].

For leukemias, $\eta = 0$ for the ERR and EAR functions. The remaining ERR parameters have means $\delta = -0.4767$, $\varphi = 0.4211$, $\log_e(\beta_M) = 0.05572$; $\log_e(\beta_F) = 0.1631$; $\gamma = -0.4011$ for ERR. For the EAR function the parameters have means $\log_e(\beta_M) = 0.485$; $\log_e(\beta_F) = -0.0703$; $\gamma = 0.2865$ and $\varphi = 0.557$.

To obtain realizations of a four-parameter beta distribution, we first compute X from applying a normal distribution with mean β_M and variance given by the first diagonal term in the ERR covariance matrix to β_M and then applying the inverse cumulative distribution function of a four-parameter gamma distribution to the so-transformed values of X.

The covariance matrices are:

CovERR(Log(β_M), Log(β_F),η, γ) = [0.031703	0.010922	0.011666	-0.021094
0.010922	0.017866	0.0094576	-0.011821
0.011666	0.0094576	0.010547	-0.023224
-0.021094	-0.011821	-0.023224	0.14091]

CovEAR(Log(β_M), Log(β_F), η, γ) = [0.029955	0.0094495	0.0093699	-0.0085991
0.0094495	0.015269	0.0086235	-0.015065
0.0093699	0.0086235	0.009300	-0.020365
-0.0085991	-0.015065	-0.020365	0.10435]

CovERR(β_M, β_F, δ, γ, φ) = [0.31306	0.24735	0.026282	0.026395	0.019503
0.24735	0.30365	0.020753	0.022953	0.015975
0.026282	0.020753	0.11003	0.016966	0.057885
0.026395	0.022953	0.016966	0.037307	0.013467
0.019503	0.015975	0.057885	0.013467	0.069669]

CovEAR(β_M, β_F, δ, γ, φ) = [0.2568	0.22277	0	0.018272	-0.0029116
0.22277	0.24963	0	0.016169	-0.0021659
0	0	0	0	0
0.018272	0.016169	0	0.021735	0.010381
-0.0029116	0.0021659	0	0.010381	0.015841]

Dose uncertainty

To accommodate dose uncertainty in the estimates of the numbers of excess cancers, we randomly drew a dose realization from a log-normal distribution that had as parameters the mean dose and the variance computed from the 0.025^{th} and 0.975^{th} quantile of the distribution for each voting precinct, age group, and race/ethnicity. To examine the impact of dose uncertainty on our 90% uncertainty intervals, we compared results for the total population (years 1945 to 2034) that accounted for all sources of uncertainty to results that did not incorporate dose uncertainty. Results are presented in Table C1.

Table C1. Impact of dose uncertainty on 90% uncertainty interval for excess cancer cases. Thus, uncertainty in dose has a substantial impact in the total population, 1945-2034.

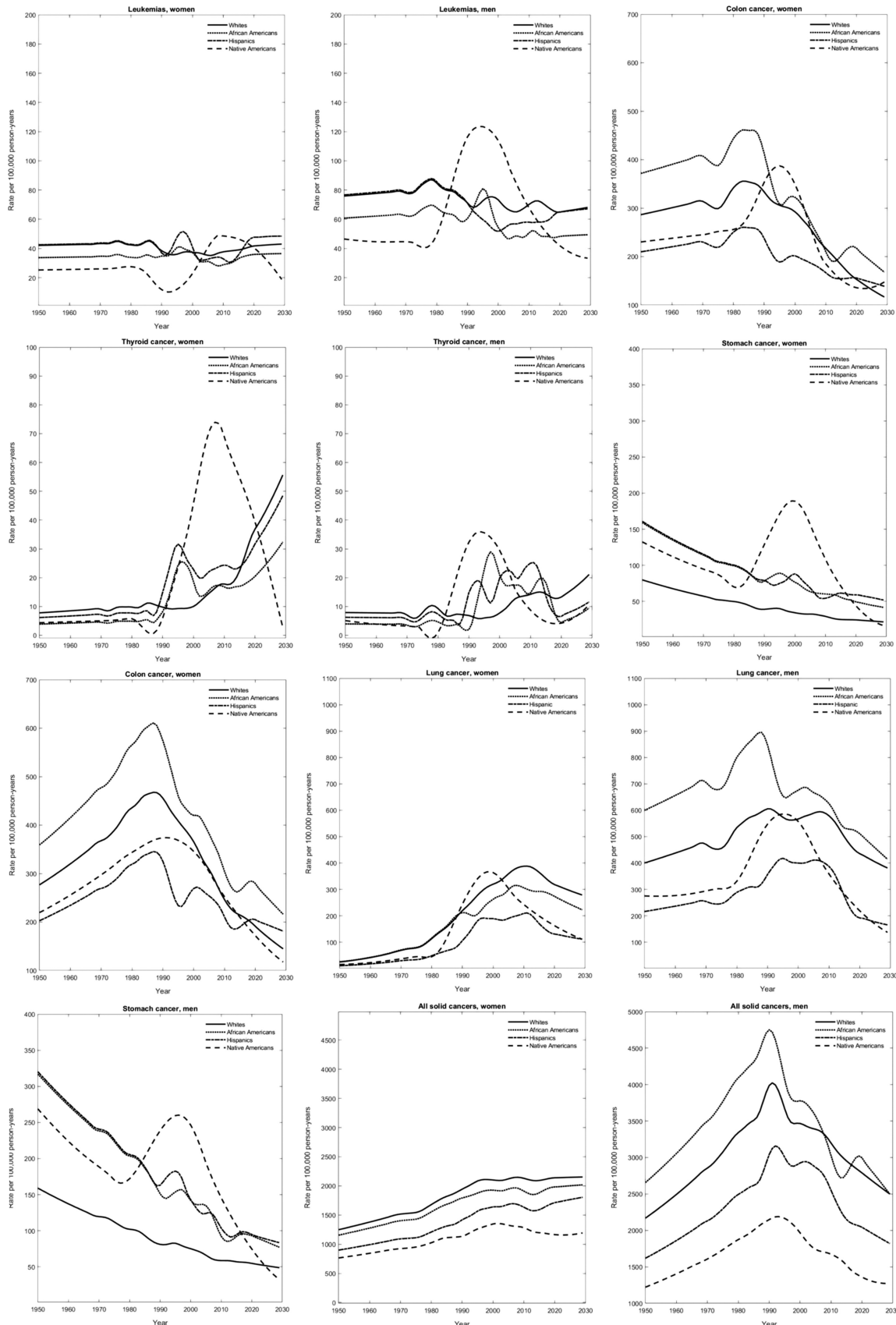| Cancer group	Length of 90% uncertainty interval (5%, 95%)		% change
	With dose uncertainty	Without dose uncertainty	
Leukemia (except CLL)	8	6	25%
Thyroid	445	224	50%
Colon	22	14	36%
Stomach	16	11	31%
Lung	41	21	49%
All Solid (except thyroid and NMSC)	246	147	40%

Fig. A1. Projected (1945-1972 2016-2034) and observed (1973-2015) baseline cancer rates per 100,000 person-years by year for individuals aged 80-84 y smoothed using loess regression.